JACS
JOURNAL OF THE AMERICAN CHEMICAL SOCIETY

ARTICLE

pubs.acs.org/JACS

A Proposal for Mitochondrial Processing Peptidase Catalytic Mechanism

Orazio Amata, Tiziana Marino, Nino Russo, and Marirosa Toscano*

Dipartimento di Chimica and Centro di Calcolo ad Alte Prestazioni per Elaborazioni Parallele e Distribuite-Centro d'Eccellenza MURST, Universita' della Calabria, I-87030 Arcavacata di Rende (CS), Italy

Supporting Information

ABSTRACT: The reaction mechanism of the Mitochondrial Processing Peptidase enzyme (MPP) was investigated by using hybrid density functional theory. This enzyme removes the NH_2-terminal targeting signals of nuclear-encoded mitochondrial protein precursors in the mitochondrial matrix. The catalytic process was studied using a model for the active site consisting of 161 atoms locating all the stationary points on the potential energy curve and determining the main energetic, structural, and electronic features that drive the catalysis. Despite the differences between the B3LYP and MPWB1K descriptions, it is possible hypothesize that the rate-limiting step of the reaction is most likely the nucleophilic attack of zinc-bound hydroxide to a carbonyl carbon of the substrate. The results allowed assignment of the proper roles to some active site residues in this mechanism.

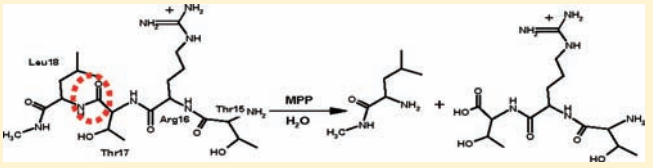

INTRODUCTION

The process of growth and division of preexisting mitochondria that give rise to new mitochondria requires a constant supply of proteins. Most of these proteins destined for the mitochondrial matrix or for the intermediate and inner membrane spaces are primarily synthesized as larger precursor polypeptides whose N-terminal extensions, which serve as the leader sequences, are proteolytically removed by specific processing peptidase enzymes during or after the precursors have been imported into mitochondria.[1] Mitochondrial Processing Peptidase (MPP; EC 3.4.24.64) is a metallopeptidase that cleaves off most of the N-terminal presequences from precursor proteins at single sites,[2,3] while the inner membrane peptidase (IMP) and mitochondrial intermediate peptidase (MIP) process only some of precursor proteins.[4]

Elimination of peptide chains presequences is required for proper protein folding: otherwise enzymes are less active and less stable thermodynamically.[4,5] The MPP, therefore, plays a crucial role in the life, hydrolyzing virtually all mitochondrial proteins from the cytoplasm. Many human diseases are related to lack of mitochondrial proteins encoded by the nucleus of the cell.[4−6] An alteration of the MPP feature leads to an accumulation of peptides precursors in the matrix that results in a slowing of cell growth and death.[7−9]

The MPP is a heterodimer enzyme that was first identified in the mitochondria of *Neurospora crassa*,[10] yeast *Saccharomyces cerevisiae*,[11] rat liver,[12] and a few plants.[13,14] Afterward, its presence was ascertained in many other organisms.[7,8,15−18] It consists of α- and β-subunits whose localization is different dependently on the considered organism. In plants, they are part of a bc1 respiratory chain complex. In yeast, one of the subunits is in the matrix while the other continues to be part of the above-mentioned bc1 complex. Finally, in animals and mushrooms they are present in the matrix.[7,8,10−18]

Both α- and β-subunits, which a crystallographic study[19] has demonstrated to have nearly identical architecture, are essential for MPP processing activity. In fact, they act cooperatively to remove the presequences from the precursor proteins. In particular, α-MPP participates in the substrate recognition through many binding sites negatively charged and present in its C-terminal domain[19−24] and a highly conserved region rich in glycine and histidine residues,[4,19,25,26] and β-MPP is the catalytic subunit.[27]

The β-subunit also contains many conserved amino acid residues that are important for substrate recognition.[3,28,29] Overall, then, the two catalytic subunits form a cavity of negative charge.[12,14,30] In addition, the walls of the cavity also contain β-sheet structures that make up a scaffold for the binding of substrate via hydrogen bonds.[14,29] This fits well with the fact that the presequences have several residues both basic (positively charged) and hydroxylated, but very rarely acidic (negatively charged).

The electrostatic interactions alone, however, do not explain the specificity of the catalytic action of MPP: it is estimated that, in mammals, the MPP processes to a single and clearly defined site over 1000 presequences which have little in common in terms of length (varying from 8 to about 69 amino acids) and primary structure. The MPP, therefore, must recognize structural elements.[18,20] In particular, the presence of distal basic residues and of one proximal to the cleavage site, connected by a region of variable length but rather flexible,[20,28,29,31−34] seems to be very important.

Many preproteins show, for the cleavage site, a pattern consisting of the sequence Rx↓ΦΨ, where ↓ indicates the bond to be hydrolyzed, R is an arginine residue, and Φ and Ψ are a hydrophobic hindered and a hydrophilic residue, respectively.[12,31−33] In some cases the arginine residue is located three amino acids

Received: July 28, 2011
Published: October 11, 2011

prior to the cleavage site, while in other cases it is positioned 10 residues away from this; finally, in about one-third of the cases, it is missing completely, indicating how the presence of this amino acid can be important but not enough to guide the action of MPP.[4,35] In fact, wide interactions between enzyme and substrate allow MPP to process with high specificity as well as those preproteins that do not fully meet all requirements for catalysis.[29]

It was demonstrated that, although β-MPP is the catalytic subunit, the recombinant subunit alone has no peptidase activity.[15,17,28,31,36,37]

The subunits of MPP also have significant sequence homology both between them and with the pitrilysin endopeptidase inverzincins family that includes *Escherichia coli* pitrilysin, the insulin degrading enzymes, the N-arginine dibasic convertase.[3,17,20,21,38]

The characteristic HXXEH amino acidic sequence typical of inverzincins is contained in the β-MPP subunit.[19] Thus, to perform its catalytic activity, the MPP requires a Zn^{2+} ion in the absence of which the enzyme is inactivated. However, other metal ions such as Mn^{2+}, Co^{2+}, Mg^{2+}, Fe^{2+}, and Ni^{2+}[14,17,18,20,38,39] seem to play a catalytic role although there is no direct evidence for this, since it is not clear whether these ions might instead play the role of effectors.

COMPUTATIONAL DETAILS

The investigation of the catalytic mechanism of the Mitochondrial Processing Peptidase (MPP) was performed at the density functional theory (DFT) level by means of the GAUSSIAN 03[40] suite of programs. Structural characterization of the transition states and intermediates along the reaction path was carried out using Becke's three-parameter hybrid exchange functional (B3)[41] in connection with the correlation functional of Lee, Yang, and Parr (LYP).[42] The potential energy profile for the reaction was determined at the same level of theory both in vacuo and in protein environments.

Different basis sets,[43] namely 6-31+G(d,p) and 6-31G(d,p), were used in the calculations for treating atoms belonging to the first and second coordination shells of a catalytic zinc ion, respectively. Instead, the Stuttgart/Dresden (SDD) quasirelativistic pseudopotential was chosen to describe the metal center.[44,45]

In order to verify if stationary points on the potential energy profile had the minimum or transition state nature, vibrational frequency analysis was done based on analytical second derivatives of the Hamiltonian at the same level of theory.

Solvent effects were introduced as single-point calculations in the framework of the self-consistent reaction field conductor-like polarizable continuum model (SCRF-CPCM)[46,47] using for the dielectric constant the empirical value of $\varepsilon = 4$ to simulate the average effect of both the protein and the water medium surrounding the protein itself.

In the CPCM method, the continuum is modeled as a conductor, instead of a dielectric. This simplifies the electrostatic computations, and corrections are made a posteriori for dielectric behavior. The UA0 radii were used to build the cavity.[48]

In order to obtain more accurate energies in the gas phase and in the protein environment, single-point calculations were performed on the B3LYP optimized geometries using the MPWB1K exchange-correlation meta-hybrid functional[49] that recent works demonstrate to be very powerful for reproducing with good accuracy experimental values in other enzymatic studies[50−52] and as able to provide kinetics features especially as far as barrier heights are concerned.[53−56]

Active Site Model. A large quantum model was built up on the basis of a recent X-ray structure of the enzyme−substrate complex where the enzyme arises from the yeast and the substrate is the peptide 2−25 of subunit IV of cytochrome oxidase (COX IV; PDB code: 1HR8).

Scheme 1. Active Site Model for Mitochondrial Processing Peptidase Enzyme[a]

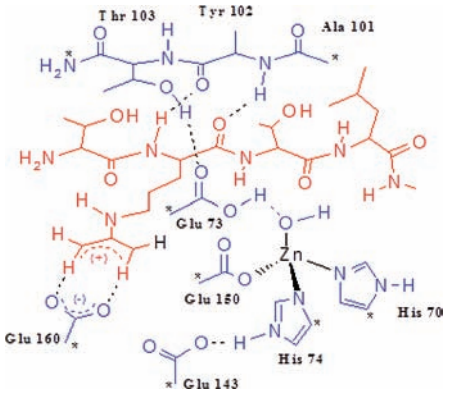

[a] Substrate is in red. Stars indicate atoms kept fixed during the optimizations.

The obtained model, having a total charge equal to −1, consists of 161 atoms (see Scheme 1) with the zinc coordinated to three amino acid residues (Glu150, His70, and His74) and to a water molecule (or an OH group) in an tetrahedral arrangement. Some second coordination shell residues (Glu73, Glu143, Glu160) and the portion of a β-sheet placed immediately above the catalytic site and interacting with the substrate complete the model. β-Sheet residues are Thr103, Tyr102, and part of Ala101. The C-terminus of the Thr103 is in the amide form, so as to simulate the peptide bond, while the Tyr102 is modeled with an alanine residue. Ala101 was truncated to the α-carbon. The nitrogen atom connected to the C-terminus end of Thr103 and the methyl carbon representative of the α-carbon of Ala101 were kept fixed in their original X-ray positions during the optimization procedure.

Substrate is a presequence of four amino acids (Thr15, Arg16, Thr17, and Leu18). Substrate N- and C- termini are given as a free amide and a methyl-amide form, respectively. No approximations were introduced as far as the tetrapeptide side chains are concerned.

Glu73 was documented as the residue that deprotonates the water molecule in the first coordination sphere of zinc. In fact, in active sites of enzymes, zinc is often bound to a water molecule involved in nucleophilic attack on a peptide carbonyl. The residue Glu160 on one side and the Thr103-Tyr102-Ala101 tripeptide on the other side keep the substrate in the right position. The Glu143 forms a salt bridge with the His74 residue.

Only the side chains of the ligands were retained; thus imidazole ring and acetate represent histidines and glutamates, respectively. To preserve the overall active site structure and to avoid artificial movements of various groups, some atoms were forced in their crystallographic positions during the optimization. These are usually the positions where the truncation of crystallographic structure is made (they are indicated by stars in Scheme 1). Using this procedure, and hence reducing the degrees of freedom of the molecular system, the model becomes slightly more rigid than it should with important effects on the energetics. However, it was demonstrated[57] that these effects usually do not alter significantly any conclusion concerning the working mechanism of the enzyme. Another consequence consists of the appearance of small imaginary frequencies, but these does not contribute to the zero-point energies (ZPE) and thus can be tolerated. However, they make the calculations of harmonic entropy effects inaccurate. Therefore, entropy was not considered in the present study.

RESULTS AND DISCUSSION

The steps involved in the whole process and determined through our calculations are sketched in Scheme 2. The potential

Scheme 2. Proposed Catalytic Cycle for Mitochondrial Processing Peptidase

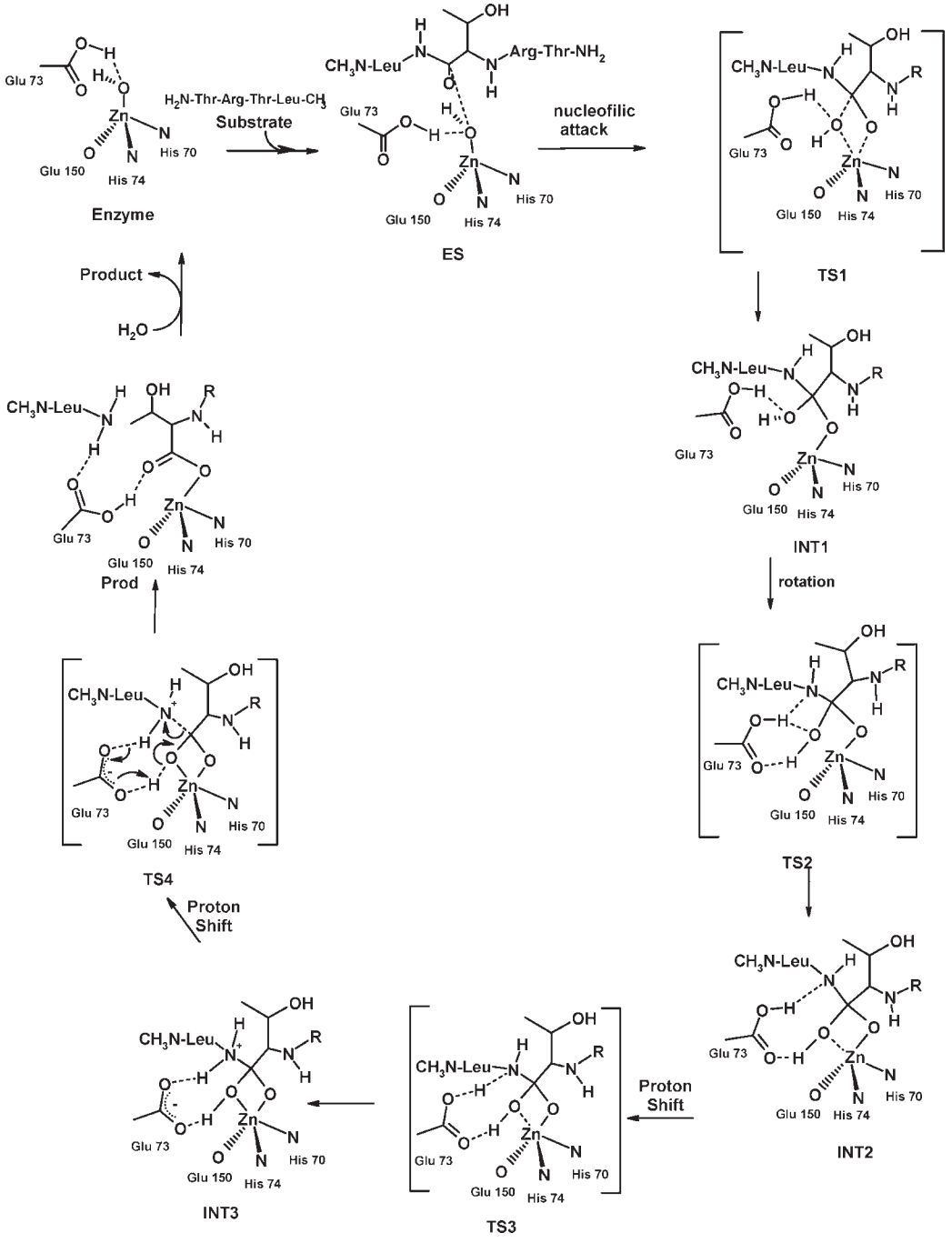

energy profile obtained in the protein environment will be the only object of the present discussion, for the considered catalytic cycle is depicted in Figure 1. Stationary point equilibrium structures are reported in Figures 2 and 3.

Optimization of the enzyme−substrate (ES) complex of MPP has allowed observation of some structural peculiarities such as the short distance, about 1.367 Å, between the zinc bound hydroxide and the proton extracted by Glu73, which suggests the likely the presence of an activated water molecule rather than a real hydroxide ion as a fourth ligand of the zinc ion, and the appearance of a hydrogen bond, little more than 2.10 Å long, between the carbonyl oxygen of Thr17 and the hydrogen atom of Leu18.

After the enzyme−substrate complex, we find the first transition state (TS1) in which the zinc bound hydroxide leads a nucleophilic attack on the substrate Thr17 carbonyl carbon (C−OH = 1.730 Å). The hydroxyl ion moves away from Zn^{2+} (Zn^{2+}−OH = 2.831 Å), and the hydrogen bond that it forms with Glu73 lengthens to about 0.2 Å. The distance between the carbonyl oxygen and amide hydrogen of Thr17 shortens to 1.932 Å, suggesting a possible stabilizing effect of the incipient negative charge on the carbonyl carbon of the substrate by this residue which thus plays a role similar to that of Tyr831 in the Insulin Degrading Enzyme (IDE).[58] From an energy point of view, the TS1 is 20.4 kcal/mol above the ES complex (Figure 1). The imaginary

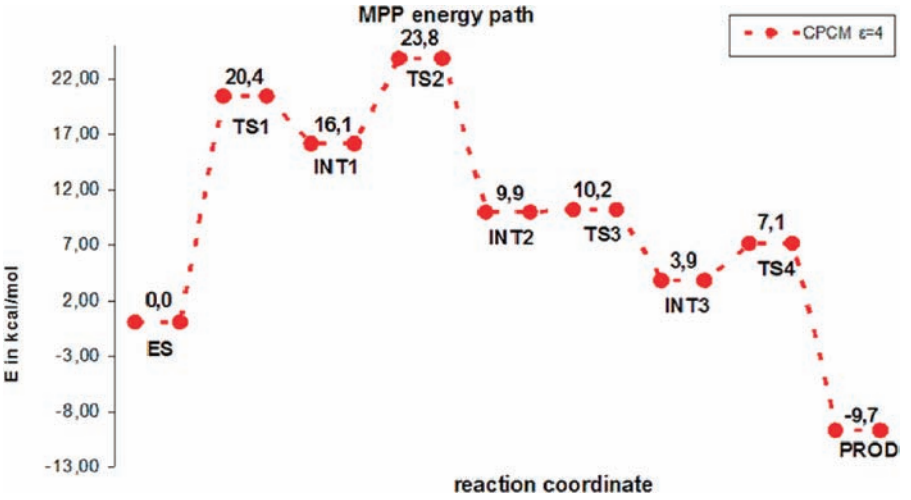

Figure 1. Energetic profile for the reaction catalyzed by MPP in protein environment.

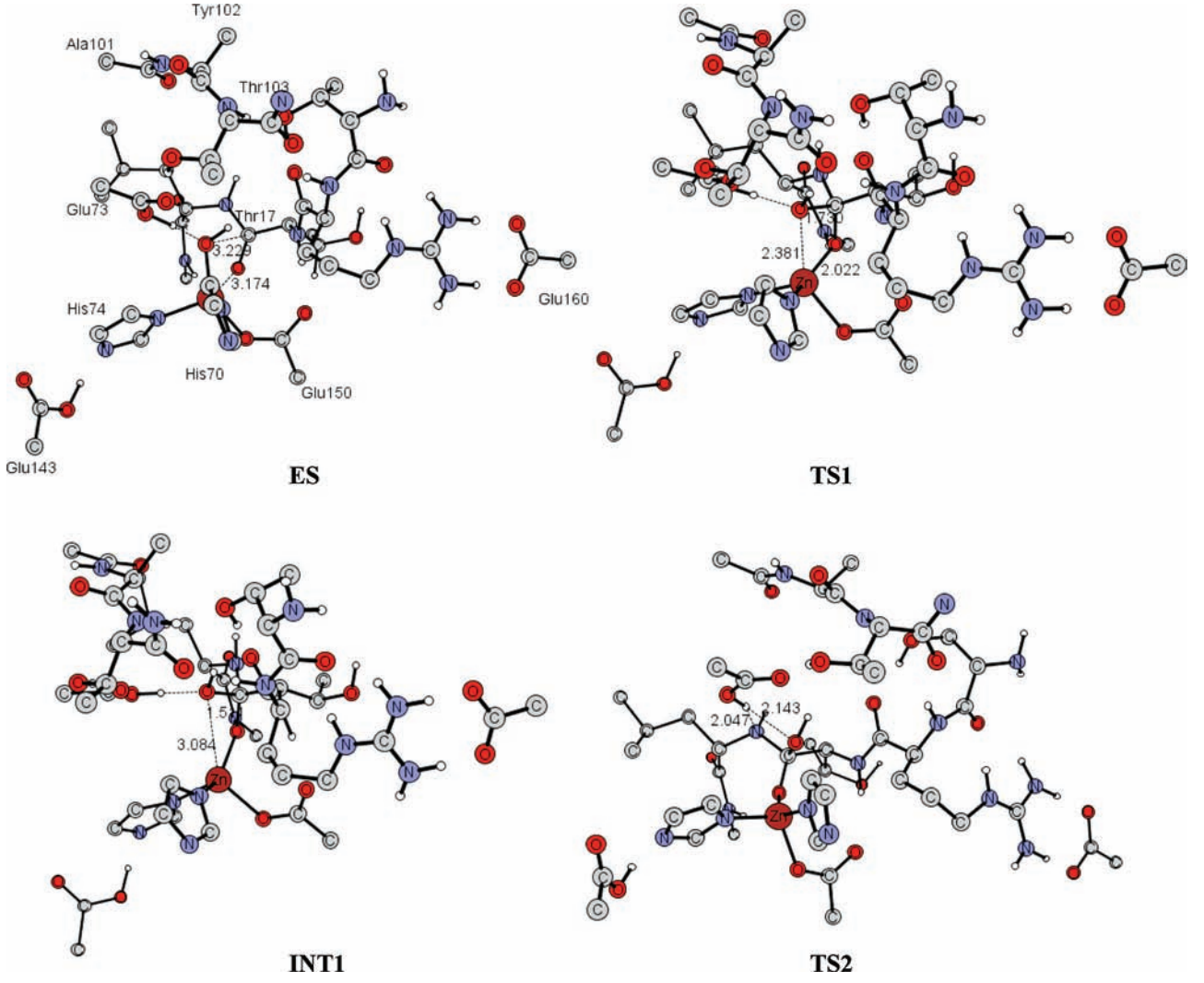

Figure 2. B3LYP optimized geometries of ES, TS1, INT1, and TS2. Only the hydrogen atoms bound to heteroatoms are reported. Distances are in Å.

vibrational frequency whose value is 213i cm^{-1} corresponds to the stretching of both Zn^{2+}—OH (that is breaking) and C—OH (that is forming) bonds.

The TS1 evolves, then, in the first intermediate (INT1) which is structurally similar to it but more stable by about 4 kcal/mol. In INT1, we can observe further lengthening

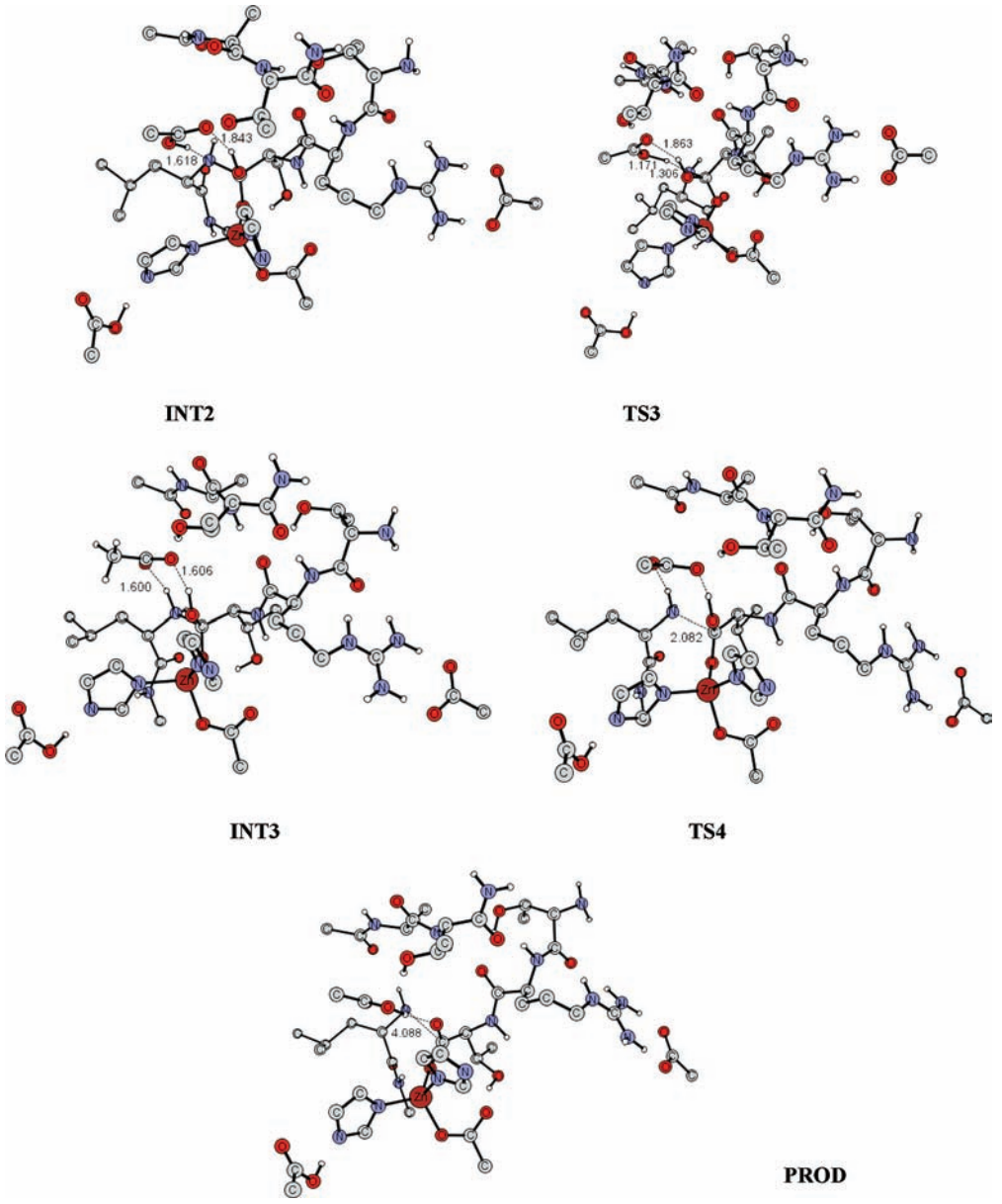

Figure 3. B3LYP optimized geometries of INT2, TS3, INT3, TS4, and PROD. Only the hydrogen atoms bound to heteroatoms are reported. Distances are in Å.

of Zn^{2+}−OH (3.084 Å) and shortening of C−OH (1.511 Å) bonds.

After INT1, it follows the second transition state (TS2) in which the hydrogen bond between Glu73 and the OH group linked to the substrate carbonyl weakens (2.143 Å) while the other two new hydrogen bonds (between the OH group of the Glu73 residue and the nitrogen atom of the leaving group (2.097 Å), and the OH group linked to the carbonyl and the other oxygen atom of the same Glu73 (2.455 Å)) begin to form. The final structure of TS2 is a consequence of the rotational movement of Glu73 which occurs at 110i cm^{-1} allowing this residue to assume a suitable orientation to give rise to the just cited interactions. TS2 lies 7.7 kcal/mol above the previous INT1.

Next to TS2, in the INT2 intermediate, the network of hydrogen bonds between the Glu73 and the substrate consolidates. Among these bonds, that between the OH group of the Glu73 residue and the nitrogen atom of the leaving group appears to be sensibly shorter (1.618 Å). The oxygen of the carbonyl does not interact more with the amide hydrogen of the Leu18 but interacts weakly with the side chain of Thr17 (2.662 Å). Energetically this structure is more stable than the previous TS2 by approximately 13.9 kcal/mol.

The next step of the mechanism involves a proton shift from Glu73 to the nitrogen atom of the leaving group to form the intermediate INT3. The third transition state TS3 is located just 0.3 kcal/mol above the preceding INT2 and occurs at the imaginary frequency of 1389i cm^{-1}.

Glu73 is now strongly hydrogen bonded (1.306 Å) to the nitrogen atom of the substrate.

In INT3, the proton of Glu73 is completely linked to the nitrogen atom of the substrate but keeps the hydrogen bond with the oxygen of the glutamate residue. This last bond is 1.600 Å long. The peptide C−N bond that must be broken appears to be

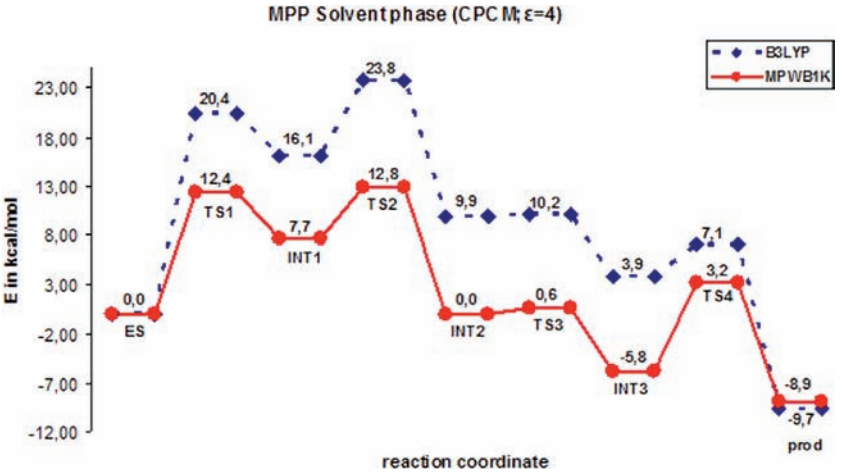

Figure 4. Comparison between B3LYP and MPWB1K energetic profiles for the reaction catalyzed by MPP enzyme.

sensibly elongated passing from a value of 1.529 Å in INT2 to 1.622 Å in INT3 while the C−OH distance shorten by about 0.05 Å. INT3 is more stable than TS3 by 6.3 kcal/mol.

The peptide bond continues to gradually grow in TS4 (2.082 Å). In addition, in TS4, the hydrogen bond between the side chain of Thr17 and the oxygen of the carbonyl loosens, to break definitively in the products. The value of the imaginary frequency at which the stretching of the peptide bond occurs is 141i cm^{-1}. From an energy point of view TS4 is approximately 3.3 kcal/mol above the INT3.

From TS4 we finally arrive at the products (PROD), where the peptide bond is hydrolyzed (4.088 Å), while the proton is transferred from the OH group of the carbonyl to the Glu73 residue.

Products are more stable on TS4 by 16.8 kcal/mol.

The reaction is exothermic to just under 10 kcal/mol. The highest barrier (20.4 kcal/mol) corresponds to the nucleophilic attack of zinc bound hydroxide to the Thr17 carbonyl of the substrate that hence represents the rate-limiting step for the process. This result is qualitatively similar to that found in the case of IDE analogous enzyme,[58] but in this case the height of the barrier falls just within the limits of the catalytic event. The Glu73 residue, as it happens in the case of IDE, acts either as a general base promoting the formation of a hydroxyl or at least activating the water molecule or as a proton shuttle favoring the expulsion of the leaving group. Instead, the role played in the IDE by Tyr831 can be played in the MPP by the main chain of the substrate and by the side chain of Thr17.

In an attempt to verify the reliability of the B3LYP energy barrier for the slowest step in the mechanism of MPP, we have performed new calculations using the MPWB1K functional that was explicitly designed for the determination of the energy barriers.[49]

The energetic profile we have obtained is reported in Figure 4 and compared with the previous B3LYP one.

As we can see the MPWB1K functional gives rise to a path systematically more favorable from a kinetic point of view (about 8 kcal), but similar to the thermodynamic one.

In particular, the barriers corresponding to the nucleophilic attack (12.4 kcal/mol) and to the Glu73 rotation (12.8 kcal/mol) differ by only 0.4 kcal/mol. The MPWB1K values of activation energies seem to be more appropriate than the B3LYP ones for a catalytic process, but the small energy difference between TS1 and TS2 in this case prevents us from identifying with certainty what is the rate-limiting step of the reaction. In fact, this can derive from the uncertainty inherent in the used method.

As far as the different evaluation of energy barriers in the two approaches is concerned we would underline that, since the new energetic values are the results of single-point calculations on the gas-phase B3LYP optimized structures, the discrepancy could come from the lack of geometry optimization.

The absence of any experimental information on the working mechanism of the studied enzyme does not help us to solve the dilemma. We, however, think that the introduction of geometry optimization in the MPWB1K computations can reduce the quantitative disagreement between the two sets of results since, despite the documented limits of the B3LYP approach, numerous studies exist that testify to its reliability in describing the enzymatic catalytic processes.[58−67]

CONCLUSIONS

In this work, we have investigated, at the density functional level of theory and in the framework of the cluster approach, the mechanism of hydrolysis of the Thr15-Arg16-Thr17-Leu18 tetrapeptide by Mitochondrial Processing Peptidase, building up an active-site model extracted from the yeast enzyme crystal structure consisting of 161 atoms and having a charge of −1.

The stationary points along the reaction path were all localized and characterized in the gas phase and protein environment. Based on these calculations, we are now able to provide a probable hypothesis of the reaction mechanism followed by MPP.

The actual process begins with the nucleophilic attack (TS1) by a zinc bound hydroxide, generated by the deprotonation of a water molecule by the Glu73 amino acid residue (ES), to a substrate carbonyl carbon. The consequent geometry reorganization that we can observe in the first intermediate (INT1) allows the key residue Glu73, which works as a shuttle, to assume the right orientation (TS2) to transfer a proton to the nitrogen atom of the peptide bond that will be hydrolyzed. In the next intermediate (INT2), this proton appears still shared between the acceptor amide nitrogen and donor Glu73 oxygen (TS3), while it is completely transferred to the nitrogen in the following step (INT3). The proton transfer weakens the C−N peptide bond (TS4) that we find definitively broken into the product (PROD).

Except for the presence of an INT3-TS4 extra step, the rest of the suggested mechanism is similar to that proposed for the IDE, an enzyme which belongs to the same inverzincins subfamily.

B3LYP computations indicate that the rate-determining step of the reaction, which is exothermic by about 10 kcal/mol, is the nucleophilic attack that entails an expense of 20.4 kcal/mol. The use of the most recent MPWB1K functional, which usually determines energy barriers with greater precision if compared to those obtained at B3LYP level and is recommended as particularly suitable for the treatment of weak interactions where B3LYP shows much less accuracy, leads to an energetic path whose stationary points, except for the product, lie about 8 kcal/mol below those obtained at the B3LYP level. The barriers for TS1 and TS2 are significantly lower but of the same order of size. For this reason we are not able to propose the rate-determining step in this case. However, the lack of geometry optimization itself suggests caution in evaluating the MPWB1K results. On the other hand, you should not underestimate the MPWB1K indication concerning the height of barriers, since the B3LYP activation energy value for the slowest step of the reaction appears to be slightly above those allowed for a catalytic process.

The role of the two most active amino acid residues in the mechanism was fully defined by our results. In particular, the Glu73 acts either as a general base generating the hydroxide nucleophile or as a proton shuttle favoring the expulsion of the leaving group. Thr17 serves to anchor the substrate and together with it stabilize the incoming negative charge that forms upon nucleophilic attack on the carbonyl carbon of the substrate.

To our knowledge, ours is the only hypothesis concerning the catalytic mechanism followed by the MPP enzyme in hydrolyzing peptide chains present in literature. We hope that it will be useful for other future theoretical and experimental investigations.

■ ASSOCIATED CONTENT

Supporting Information. Experimental details and complete ref 40. This material is available free of charge via the Internet at http://pubs.acs.org.

■ AUTHOR INFORMATION

Corresponding Author
m.toscano@unical.it

■ ACKNOWLEDGMENT

We gratefully acknowledge the Dipartimento di Chimica, Università della Calabria for financial aid.

■ REFERENCES

(1) Zhang, X.-P.; Sjöling, S.; Tanudji, M.; Somogyi, L.; Andreu, D.; Göran Eriksson, L. E.; Gräslund, A.; Whelan, J.; Elzbieta Glaser, E. *Plant J.* **2001**, *27*, 427.
(2) Song, M.-C.; Shimokata, K.; Kitada, S.; Ogishima, T.; Ito, A. *J. Biochem.* **1996**, *120*, 1163.
(3) Kitada, S.; Kojima, K.; Shimokata, K.; Ogishima, T.; Ito, A. *J. Biol. Chem.* **1998**, *49*, 32547.
(4) Gakh, O.; Cavadini, P.; Isaya, G. *Biochim. Biophys. Acta* **2002**, *1592*, 63.
(5) MacKenzie, J. A.; Payne, R. M. *Biochim. Biophys. Acta* **2007**, *1772*, 509.
(6) Mukhopadhyay, A.; Yang, C.-S.; Wei, B.; Weiner, H. *J. Biol. Chem.* **2007**, *282*, 37266.
(7) Géli, V.; Yang, M.; Suda, K.; Lustig, A.; Schatz, G. *J. Biol. Chem.* **1990**, *265*, 19216.
(8) Witte, C.; Jensen, R. E.; Yaffe, M. P.; Schatz, G. *EMBO J.* **1988**, *7*, 1439.
(9) Jensen, R. E.; Yaffe, M. P. *EMBO J.* **1988**, *7*, 3871.
(10) Hawlitschek, G.; Schneider, H.; Schmidt, B.; Tropschug, M.; Hartl, F.-U.; Neupert, W. *Cell* **1988**, *53*, 795.
(11) Yang, M.; Jensen, R. E.; Yaffe, M. P.; Opplinger, W.; Schatz, G. *EMBO J.* **1988**, *7*, 3857.
(12) Ou, W.-J.; Ito, A.; Okazaki, H.; Omura, T. *EMBO J.* **1989**, *8*, 2605.
(13) Eriksson, A. C.; Glaser, E. *Biochim. Biophys. Acta* **1992**, *1140*, 208.
(14) Braun, H.-P.; Emmermanm, M.; Kruft, V.; Schmitz, U. K. *EMBO J.* **1992**, *9*, 3219.
(15) Jensen, R. E.; Yaffe, M. P. *EMBO J.* **1988**, *7*, 3863.
(16) Braun, H.-P.; Schmitz, U. K. *Int. J. Biochem. Cell Biol.* **1997**, *29*, 1043.
(17) Kleiber, J.; Kalousek, F.; Swaroop, M.; Rosenberg, L E. *Proc. Natl. Acad. Sci. U.S.A.* **1990**, *87*, 7978.
(18) Bohni, P. C.; Daum, G.; Schatz, G. *J. Biol. Chem.* **1983**, *258*, 4937.
(19) Taylor, A. B.; Smith, B. S.; Kitada, S.; Kojima, K.; Miyaura, H.; Otwinowski, Z.; Ito, A.; Deisenhofer, J. *Structure* **2001**, *9*, 615.
(20) Yang, M.; Géli, V.; Oppliger, W.; Suda, K.; James, P.; Schatz, G. *J. Biol. Chem.* **1991**, *266*, 6416.
(21) Shimokata, K.; Kitada, S.; Ogishima, T.; Ito, A. *J. Biol. Chem.* **1998**, *273*, 25158.
(22) Gakh, O.; Obsil, T.; Adamec, J.; Spizek, J.; Amler, E.; Janata, J.; Kalousek, F. *Arch. Biochem. Biophys.* **2001**, *385*, 392.
(23) Janata, J.; Holá, K.; Kubala, M.; Gakh, O.; Parkhomenko, N.; Matušková, A.; Kutejová, E.; Amler, E. *Biochem. Biophys. Res. Commun.* **2004**, *316*, 211.
(24) Kojima, K.; Kitada, S.; Shimokata, K.; Ogishima, T.; Ito, A. *J. Biol. Chem.* **1998**, *273*, 32542.
(25) Maskos, K. Pitrilysins/Inverzincins. In *Handbook of Metalloproteins*; Messerschmidt, A., Dode, W., Cygler, M., Eds.; Jonh Wiley & Sons: 2004.
(26) Paetzel, M.; Karla, A.; Strynadka, N. C. J.; Dalbey, R. E. *Chem. Rev.* **2002**, *102*, 4549.
(27) Nagayama, K.; Itono, S.; Yoshida, T.; Ishiguro, S.-I.; Ochiai, H.; Ohmachi, T. *Biosci. Biotechnol. Biochem.* **2008**, *72*, 1836.
(28) Kitada, S.; Kojima, K.; Ito, A. *Biochem. Biophys. Res. Commun.* **2001**, *287*, 594.
(29) Kitada, S.; Yamasaki, E.; Kojima, K.; Ito, A. *J. Biol. Chem.* **2003**, *278*, 1879.
(30) Shimokata, K.; Kitada, S.; Ogishima, T.; Ito, A. *J. Biol. Chem.* **1998**, *273*, 25158.
(31) Arretz, M.; Schneider, H.; Guiard, B.; Brunner, M.; Neupert, W. *J. Biol. Chem.* **1994**, *269*, 4959.
(32) Sjöling, S.; Eriksson, A. C.; Glasier, E. *J. Biol. Chem.* **1994**, *269*, 32059.
(33) Rudhe, C.; Clifton, R.; Chew, O.; Zeman, K.; Richter, S.; Lamppaa, G.; Whelam, J.; Glaser, E. *J. Mol. Biol.* **2004**, *343*, 639.
(34) Kojima, K.; Kitada, S.; Ogishima, T.; Ito, A. *J. Biol. Chem.* **2001**, *276*, 2115.
(35) Waltner, M.; Weiner, H. *J. Biol. Chem.* **1995**, *270*, 26311.
(36) Gèli, V. *Proc. Natl. Acad. Sci. U.S.A.* **1993**, *90*, 6247.
(37) Saavedra-Alanis, V. M.; Rysavy, P.; Rosenberg, L. E.; Kalousek, F. *J. Biol. Chem.* **1994**, *269*, 9284.
(38) Schneider, H.; Arretz, M.; Wachter, E.; Neupert, W. *J. Biol. Chem.* **1990**, *265*, 9881.
(39) Deng, K.; Zhang, L.; Kachurin, A. M.; Yu, L.; Xia, D.; Kim, H.; Deisenhofer, J.; Yu, C.-A. *J. Biol. Chem.* **1998**, *273*, 20752.
(40) Frisch, M. J., et al. *Gaussian 03*; Gaussian, Inc.: Pittsburgh, PA, 2003.
(41) Becke, A. D. *J. Chem. Phys.* **1993**, *98*, 5648.
(42) Lee, C. T.; Yang, W. T.; Parr, R. G. *Phys. Rev. B: Condens. Matter Mater. Phys.* **1988**, *37*, 785.

(43) Becke, A. D. *Phys. Rev. B* **1988**, *38*, 3098.
(44) Dolg, M.; Wedig, U.; Stoll, H.; Preuss, H. *J. Chem. Phys.* **1987**, *86*, 866.
(45) Andrae, D.; Haussermann, U.; Dolg, M.; Stoll, H.; Preuss, H. *Theor. Chim. Acta* **1990**, *77*, 123.
(46) Barone, V.; Cossi, M. *J. Phys. Chem. A* **1998**, *102*, 1995.
(47) Cossi, M.; Rega, N.; Scalmani, G.; Barone, V. *J. Comput. Chem.* **2003**, *24*, 669.
(48) Rappe, A. K.; Casewit, C. J.; Colwell, K. S.; Goddard, W. A., III; Skiff, W. M. *J. Am. Chem. Soc.* **1992**, *114*, 10024.
(49) Zhao, Y.; Truhlar, D. G. *J. Phys. Chem. A* **2004**, *108*, 6908.
(50) Schenk, G.; Ge, Y.; Carrington, L. E.; Wynne, C. J.; Searle, I. R.; Carroll, B. J.; Hamilton, S.; de Jersey *J. Arch. Biochem. Biophys.* **1999**, *370*, 183.
(51) Schenk, G.; Gahan, L. R.; Carrington, L. E.; Mitić, N.; Valizadeh, M.; Hamilton, S. E.; de Jersey, J.; Guddat, L. W. *Proc. Natl. Acad. Sci. U.S.A.* **2005**, *102*, 273.
(52) Cox, R. S.; Schenk, G.; Mitic, N.; Gahan, L. R.; Hengge, A. C. *J. Am. Chem. Soc.* **2007**, *129*, 9550.
(53) Sousa, S. F.; Fernandes, P. A.; Ramos, M. J. *J. Phys. Chem. A* **2007**, *111*, 10439.
(54) Bras, N. F.; Moura-Tamames, S. A.; Fernandes, P. A.; Ramos, M. J. *J. Comput. Chem.* **2008**, *29*, 2565.
(55) Leopoldini, M.; Russo, N.; Toscano, M. *Chem.—Eur. J.* **2009**, *15*, 8026.
(56) Alberto, M. E.; Marino, T.; Ramos, M. J.; Russo, N. *J. Chem. Theory Comput.* **2010**, *6*, 2424.
(57) Chen, S.-L.; Fang, W.-H.; Himo, F. *Theor. Chem. Acc.* **2008**, *120*, 515.
(58) Amata, O; Marino, T.; Russo, N.; Toscano, M. *J. Am. Chem. Soc.* **2009**, *131*, 14804.
(59) Leopoldini, M.; Russo, N.; Toscano, M. *J. Phys. Chem. B* **2006**, *110*, 1063.
(60) Marino, T.; Russo, N.; Toscano, M. *J. Am. Chem. Soc.* **2005**, *127*, 4242.
(61) Siegbahn, P. E. M.; Blomberg, M. R. A. *Chem. Rev.* **2000**, *100*, 421.
(62) Noodleman, L.; Lovell, T.; Han, W. G.; Li, J.; Himo, F. *Chem. Rev.* **2004**, *104*, 459.
(63) Leopoldini, M.; Russo, N.; Toscano, M. *J. Am. Chem. Soc.* **2007**, *129*, 7776.
(64) Leopoldini, M.; Russo, N.; Toscano, M.; Dulak, M.; Wesoloski, A. T. *Chem.—Eur. J.* **2006**, *12*, 2532.
(65) Leopoldini, T.; Marino, N.; Toscano, M. *Theor. Chem. Acc.* **2008**, *120*, 459.
(66) Ramos, M. J.; Fernandes, P. A. *Acc. Chem. Res.* **2008**, *41*, 689.
(67) Russo, N.; Leopoldini, M.; Toscano, M. *Chem.—Eur. J.* **2007**, *13*, 2109.